Journal of Cellular Biochemistry 97:1036–1051 (2006)

Tumor Metastasis in an Orthotopic Murine Model of Head and Neck Cancer: Possible Role of TGF-Beta 1 Secreted by the Tumor Cells

Santanu Dasgupta,[1] Malaya Bhattacharya-Chatterjee,[1] Bert W. O'Malley, Jr.,[2] and Sunil K. Chatterjee[1]*

[1]Department of Internal Medicine and the Barrett Cancer Center, University of Cincinnati, Cincinnati, Ohio 45267-0509

[2]Department of Otolaryngology, Head and Neck Surgery, University of Pennsylvania Health System, Philadelphia, Pennsylvania 19104-4283

Abstract In an orthotopic murine model of head and neck cancer, combined subcutaneous and intratumoral vaccination with recombinant vaccinia virus expressing interleukin-2 (rvv-IL-2) induced significant tumor regression early on therapy. However, its efficacy was restricted by recurrent tumor growth and loco-regional metastases. In this study, we explored the mechanism of tumor metastasis. We compared the levels of expression of a number of molecules involved in tumor metastasis, which included transforming growth factor-β1 (TGF-β1), E-cadherin, matrix metalloproteinases (MMPs): MT1-MMP, MMP-2, MMP-9, their tissue inhibitors (TIMPs): TIMP-1/TIMP-2, and pro-angiogenic factors CD31, VEGF-R2, and iNOS between primary and metastatic tumors by real-time RT-PCR and immunohistochemistry. We detected spontaneous lymph node and tongue metastasis. Metastasis was delayed in rvv-IL-2 treated mice. Cultured tumor cells expressed negligible amount of TGF-β1. Untreated or metastatic tumors, on the other hand, expressed high levels of TGF-β1 and secreted TGF-β1 in the sera of tumor-bearing mice. Levels of TGF-β1 in the sera suddenly jumped at the time when tumor metastasis started. In the metastatic tumors, levels of MT1-MMP, MMP-2, and MMP-9 were significantly elevated ($P < 0.001$), while levels of TIMP-1/TIMP-2 and E-cadherin were decreased ($P < 0.001$) compared to control or primary tumors. Levels of CD31, VEGF-R2, and iNOS were also significantly elevated in the metastatic lesions ($P < 0.001$). The concurrence of high levels of TGF-β1 in the sera, expression of proteins involved in metastasis and initiation of metastasis suggested possible role of TGF-β1 in on setting the metastatic cascade in this model. J. Cell. Biochem. 97: 1036–1051, 2006.

Key words: head and neck cancer; metastasis; TGF-beta 1

Head and neck squamous cell carcinoma (HNSCC) is one of the most prevalent cancer types worldwide with more than 500,000 annual incidences [Kim et al., 2002]. It is the fifth leading cause of cancer incidence and sixth leading cause of cancer related death [Kim et al., 2002]. In the United States, it accounts for 6% of all cancer diagnosed and results in an estimated 14,000 deaths annually [Edwards et al., 2002]. Despite significant advancement in the therapeutic regimens for treating HNSCC, 5-year survival rate remained poor over the last 20 years [Edwards et al., 2002; Kim et al., 2002]. The major contributing factors for low survival include loco-regional relapse, lymph node and distant metastatic spread of the primary tumor [Werner et al., 2002; Ginos et al., 2004]. Patients with recurrent or metastatic HNSCC have median survival rate of approximately 6 months [Kim et al., 2002]. For treating recurrent HNSCC tumors, therapy utilizing different growth regulatory cytokines, particularly interleukin-2 showed promise [Li et al., 1999; De Stefani et al., 2002]. However, management of distant metastatic remains a major problem.

Grant sponsor: National Cancer Institute (NIH); Grant number: RO1CA89748.

*Correspondence to: Prof. Sunil K. Chatterjee, PhD, Department of Medicine, The Vontz Center for Molecular Studies, University of Cincinnati, 3125 Eden Avenue, Cincinnati, OH 45267-0509.

E-mail: sunil.chatterjee@uc.edu

Received 18 May 2005; Accepted 18 August 2005

DOI 10.1002/jcb.20647

Tumor metastasis is a complex process consisting of loss of tumor cell adhesion, extracellular matrix (ECM) proteolysis including basement membrane and subsequent cell migration within the surrounding microenvironment. In epithelial tissues, cell–cell adhesion is mediated largely by the members of the cadherin family and in particular by E-cadherin which forms the key functional component of adherence junction between epithelial cells [Rodrigo et al., 2002]. Cadherins are a family of calcium dependent cell adhesion molecules, which mediate predominantly homotypic cell–cell interactions and play a key role during morphogenesis as well as in the maintenance of the differentiated phenotypes [Rodrigo et al., 2002].

Among the proteinases contributing to the degradation of ECM, the family of matrix metalloproteinases (MMPs) plays a significant role in tumor invasion and metastasis [Huang et al., 2001; Werner et al., 2002] and plays a major role in the disease progression and death of cancer patients. Basement membrane degradation helps in tumor growth, angiogenesis, local invasion, and subsequent distant metastasis [Chambers and Matrisian, 1997; Werner et al., 2002]. MMPs belong to a rapidly growing family of zinc-dependent endopeptidases capable of degrading a variety of ECMs [Chambers and Matrisian, 1997; Huang et al., 2001; Werner et al., 2002; Hofmann et al., 2003]. In general MMPs are secreted in latent forms (Pro-MMPs) and required specific proteolytic activation [Nagase, 1997]. Among different MMPs, overexpression of MT1-MMP, MMP-2, and MMP-9 in particular has been correlated with increased tumor invasion in different tumor types [Huang et al., 2001; Hofmann et al., 2003; Trudel et al., 2003; Lu et al., 2004a] including HNSCC [Franchi et al., 2002; Werner et al., 2002]. Activity of these MMPs is regulated at several levels including transcription, translation, extracellular activation and finally by specific tissue inhibitors of MMPs known as TIMPs [Franchi et al., 2002; Werner et al., 2002]. Of the TIMPs, TIMP-1 and TIMP-2 are the best characterized inhibitors of all known MMPs [Kim et al., 2000]. TIMP-2 in particular regulates the activity of the above three MMPs in a concentration dependent manner [Lu et al., 2004a].

Metastatic potential of the tumor cells has also been shown to be correlated with the expression levels of several angiogenic genes including vascular endothelial growth factor (VEGF) and one of its receptors, vascular endothelial growth factor-receptor 2 (VEGF-R2), which are critical for promoting angiogenesis in different tumor types including HNSCC [Sauter et al., 1999; Basu et al., 2001; Huang et al., 2001]. Studies performed on different tumor types including HNSCC, have also demonstrated that inducible nitric oxide synthase (iNOS) and NO levels are increased significantly in tumor tissues compared to the normal and this event appears to be crucial for invasion and angiogenesis [Franchi et al., 2002]. Although the mechanisms of action of NO that are involved in the process of local invasion and metastasis are defined poorly, studies conducted on joint disease as well as on a murine mammary tumor model have indicated that NO can induce the expression of MMP family members [Franchi et al., 2002].

TGF-β superfamily consists of multifunctional cytokines that regulate cell growth and differentiation, tissue remodeling, immune response, and angiogenesis [Yang et al., 2002]. Among these, TGF-β1 in particular has been reported to be overexpressed in many types of cancer and implicated in fibro-proliferative disorders, immunosuppression, tumor invasion and metastasis [Yang et al., 2002; Lu et al., 2004b]. It has also been suggested that TGF-β1 promotes tumor invasion via its paracrine effect on tumor stroma [Yang et al., 2002; Lu et al., 2004b]. However, it is not clear at which stage of HNSCC development TGF-β1 overexpression begins and the role of TGF-β1 in HNSCC carcinogenesis remains to be determined [Lu et al., 2004b].

We have previously demonstrated efficient tumor regression in an orthotopic murine model of HNSCC treated with recombinant vaccinia virus expression IL-2 [Dasgupta et al., 2003]. Despite significant tumor regression, vaccine efficacy appeared to be restricted by recurrence and loco-regional metastasis of the primary tumor. In this study, we explored the molecular mechanism of metastasis in order to improve our vaccination strategy by arresting tumor metastasis.

MATERIALS AND METHODS

Animals and Reagents

We obtained C3H/HeJ, female mice from Jackson Laboratories (Bar Harbor, ME). Tissue

culture media and reagents were purchased from Life Technologies, Inc. (Gaithersburg, MD). We procured the following rabbit anti-mouse polyclonal antibodies from Chemicon International (Temecula, CA): anti-MT1-MMP (# AB851), anti-MMP-2 (#AB809), anti-MMP-9 (#AB19047), anti-TIMP-1 (#AB800), anti-TIMP-2 (#AB19029), anti-iNOS (#AB5382), and rabbit IgG (#AP132B). Purified anti-CD31, anti-VEGF-R2 (Flk-1), biotinylated anti-rat IgG antibodies, and streptavidin-HRP kits were purchased from BD Pharmingen (San Diego, CA). Anti E-cadherin and TGF-β1 antibodies (MAB 1835, AB-246-NA, and AF-101-NA) and TGF-β1 ELISA kit were purchased from R&D systems (Minneapolis, MN). All PCR primers were procured from Integrated DNA Technologies (Coralville, IA).

Immunotherapy With Recombinant Vaccinia Virus

We used recombinant vaccinia virus (rvv) expressing IL-2 (rvv-IL-2) and control rvv, rvv-lacZ expressing *Escherichia coli* β-galactosidase for the preparation of the vaccines. The procedures for the preparation of rvv-IL-2 and rvv-lacZ have been described previously [Qin and Chatterjee, 1996]. For mock vaccination, we used 100 μL of PBS (10 mM phosphate buffer, pH 7.2, 0.15 M NaCl) and injected in the flank or at the tumor site of the mice as appropriate.

We cultured murine SCCVII/SF tumor cells in Dulbecco's modified Eagle's medium containing 10% fetal calf serum, 100 U/ml penicillin, 100 μg/ml amphotericin B, and 2 mM L-glutamate. For the development of oral tumor, we anesthetized syngeneic C3H/HeJ mice with 3% isoflurane (Abbott Laboratories, Chicago, IL) and then injected SCCVII/SF cells (1×10^5) slowly into the floor of mouth of the mouse with a 23-gauge needle at the depth of mylohyoid muscle [Dasgupta et al., 2003]. All procedures were performed in accordance with the University of Cincinnati Institutional Guidelines for the care and use of laboratory animals.

Mice received subcutaneous injection of irradiated, rvv-infected SCC VII/SF cells and intratumoral vaccination with rvv, at the same time. The control group received rvv-lacZ instead of rvv-IL-2. For s.c. vaccination, we irradiated monolayers of SCCVII/SF cells with a total of 10,000 rad of γ-radiation (Cesium-167). The cells were then infected with 1×10^5 pfu/ml rvv. After 24 h of infection, we injected 1×10^4 cells in 100 μL PBS subcutaneously into the left flank of the mice. For intratumoral vaccination, 1×10^9 pfu (plaque forming units) of either rvv-IL-2 or rvv-lacZ were injected directly into the tumor in 100 μL of PBS. We prepared and injected the tumor cells as above on day 0. First vaccination was given on day 7 when tumor weight reached 40–50 mg. Subsequent vaccinations were given on days 10 and 14.

Tumor Growth and Metastasis

We daily monitored the tumor growth. Mice showing signs of morbidity according to the Institutional Animal Care and Use Committee protocol were immediately sacrificed. Following sacrifice mean tumor weight was determined from at least four mice from each group. We isolated superficial cervical (four nodes), deep cervical (two nodes), and mediastinal (two nodes) lymph nodes surrounding the oral cavity from each mouse on day 9, 12, 16, 20, and 25. For detecting metastatic tumor nest, different lymph nodes from several mice of each vaccinated group were embedded in paraffin, sectioned (5 μm) and stained with Harry's Hematoxyline and Eosin. Lymph nodes from different treated groups were also cultured in complete DMEM medium to verify tumor cell infiltration. Positive lymph nodes were scored only after microscopic examination of several lymph nodes from a number of mice in each group as well as from the positive lymph node cultures. We also examined floor of mouth, palate, buccal mucosa, oropharynx, tongue, lung, liver, spleen, and kidney on different days for visible metastasis and also examined serial section from these regions for possible tumor invasion. Invasive tumor cells were identified based on the morphology of the SCCVII/SF tumor cells.

Immunohistochemistry

To study the expression of MT1-MMP, MMP-2, MMP-9, TIMP-1, TIMP-2, E-cadherin, CD31, VEGF-R2, iNOS, and TGF-β1, we used both fresh frozen and paraffin embedded primary and metastatic tumor tissues collected on day 16 and 25. Several tumor sections from different regions of the tumors were stained and examined for the determination of protein expression. Staining was performed as described earlier [Dasgupta et al., 2004]. For counting of the positively stained cells or intensity measurement we used Metamorph software

(Universal Imaging, Downington, PA) as described earlier [Dasgupta et al., 2004]. At least 10 fields were chosen at random for counting and data are expressed as mean ± SE. For intensity measurement, lowest value (≤50) was represented by a single + sign and each fold increase was represented by additional + - sign [Dasgupta et al., 2004]. For comparison all sections were processed in parallel. At least five tumors from five mice of each group were analyzed to confirm the results.

Quantitative Real Time RT-PCR Analysis

Total RNA was prepared from tumor tissues of mice as described earlier [Qin et al., 2001]. For quantitative analysis, total RNA extracted was subjected to real-time RT-PCR using Cepheid Smart Cycler system (Sunnyvale, CA) in triplicate. The sequence of all the primers were as follows: MMP-2: forward 5′-TAGTGATGGTTCCCCTCCTC-3′, reverse 5′-TACTTGTTTGCCATTTCCCA-3′, MMP-9: forward 5′-CTCTCTACTGGGCGTTAGGG-3′, reverse 5′-TGAGTGAGTTGGACTCTCGG-3′, TIMP-1: forward 5′-CGAATCAACGAGACCACCTTATACC-3′, reverse 5′-CTGGAGAGTGACACTCACTGTTTG-3′, TIMP-2: forward 5′-CACAGACTTCAGCGAATGGA-3′, reverse 5′-CTTGGGAAGCTTGAGAGTGG-3′ and E-cadherin: forward 5′-GACTGGGTCATCCCTCCCATCAGCTGCCCCGA-3′, reverse 5′-AGGAGCGTTGTCATTAATATCCTTGAC-3′. Real-time RT-PCR analysis was performed as described earlier [Dasgupta et al., 2004]. Before analysis of the target genes, expression level of the internal control β-actin in all samples was normalized with respect to the threshold cycle number (C_t). Relative fold number of the target gene was then expressed with respect to the normalized internal control β-actin in each case. PCR reaction was carried out in 20 μL reaction volume using SYBR Green QuantiTect RT-PCR kit (Qiagen, Valencia, CA) as described earlier [Dasgupta et al., 2004]. Briefly, reverse transcription was carried out at 50°C for 20–30 min. Inactivation of reverse transcriptase, HotStarTaq DNA polymerase activation and template cDNA denaturation were carried out at 95°C for 15 min. The final cDNA amplification step comprised of 40 cycles at 94°C for 30 s, 52°C for 30 s, and 72°C for 1 min. Data analysis was done using $2^{-\text{deltadelta}}$ C_t method as described earlier [Dasgupta et al., 2004]. Relative fold number of the target gene expression was determined by subtracting the C_t value of the reference gene from the C_t value of target gene in all cases.

ELISA for TGF-β1

Amounts of TGF-β1 in the sera of PBS or rvv-IL-2 vaccinated mice were measured on days 3, 6, 9, 12, 15, 18, 21, and 24 by ELISA kits (R&D Systems). Naïve mice were used as control. Before ELISA, serum was mixed with 2.5 N acetic acid, 10 M urea, and incubated at room temperature for 10 min according to the manufacturer's instruction to obtain active form of TGF-β1. Neutralization was performed with 2.7 N NaOH, 1 M HEPES. All experiments were performed in triplicate. The lower limit for the cytokine detection was 5 pg/ml.

Statistical Analysis

We used Student's *t*-test for normally distributed variables. When the data did not fulfill the criteria of being normally distributed, we used nonparametric statistics (Mann–Whitney rank sum test). We performed all statistical evaluation using SigmaStat software (Jandel, San Rafael, CA) and considered $P < 0.05$ to indicate statistical significance

RESULTS

Effect of rvv-IL-2 Vaccination on Established Oral Tumor and Subsequent Metastasis of the Primary Tumor Into the Lymph Nodes and Tongue

In an established orthotopic oral tumor model we tested the efficacy of rvv-IL-2 vaccination. Therapy was started when tumor became 40–50 mg. Combined subcutaneous and intratumoral rvv-IL-2 vaccinations were administered on days 7, 10, and 14. By this vaccination strategy, we achieved significant tumor growth inhibition by day 12 in the rvv-IL-2 vaccinated mice compared to the controls (Fig. 1A). By day 12, tumor sizes were 53 ± 4 mg in the rvv-IL-2 vaccinated group compared to 123 ± 14 mg in rvv-lacZ treated mice ($P < 0.0001$). We could not compare further the tumor growth between different groups since all mice from control rvv-lacZ group died by this time although further tumor regression was observed in rvv-IL-2 group by day 16 when tumor weight became 26 ± 4 mg, nearly half the size of the initial tumor weight at the start of therapy (Fig. 1A). However, we did not detect any further regression; instead tumor size increased to 46 ± 5 mg

on day 25 and all mice became moribund (Fig. 1A) and further rvv-IL-2 vaccination did not improve the situation. One possibility is that the recurrent tumor growth and failure of the vaccine to eradicate the tumor are due to tumor metastasis into the regional lymph nodes and local organs. To test this possibility, we isolated 8 accessible lymph nodes from individual mouse of the different vaccinated groups surrounding the oral tumor and checked for possible infiltration by tumor cells. Results shown in Figure 1B indicated that in the PBS group by day 9, all the mice were positive for tumor infiltration in 5–8 lymph nodes, while in the rvv-lacZ vaccinated group on that day, all the mice were positive for tumor infiltration involving 4–7 lymph nodes. However, all the rvv-IL-2 vaccinated mice were free from any lymph node metastasis on day 9. All mice in the PBS group died by day 9. On day 12, in the rvv-lacZ vaccinated group all the 4 mice were positive for tumor infiltration into almost all the 8 lymph nodes (Fig. 1B). At this point, 4/7 mice in the rvv-IL-2 vaccinated group were positive for tumor infiltration into 1–2 lymph nodes. All rvv-lacZ vaccinated mice died before day 16. Whereas, despite significant tumor regression by day 16 in rvv-IL-2 vaccinated mice, 6/7 of the mice were positive for tumor infiltration involving 2–4 lymph nodes. We did not observe any further tumor regression, and by day 25, lymph node metastasis was evident in all 5 rvv-IL-2 treated mice involving 6-8 lymph nodes. Histopathologic evidence of the presence of infiltrated tumor nests in different lymph nodes of the rvv-IL-2 vaccinated groups on day 25 was shown in Figure 1C.

Apart from regional lymph nodes, metastasis of oral tumor into the local organs such as floor of mouth, tongue, palate, oropharynx, larynx is a frequent event in the human HNSCC [Kim et al., 2002; Werner et al., 2002]. Since this model closely resembles human HNSCC, migration of tumor cells into these sites is possible. To test this possibility we examined these regions for metastatic invasion. As shown in Figure 2, we detected tongue metastasis as early as by day 16 in the rvv-IL-2 vaccinated mice. Invasion of tumor into the tongue epithelium (Fig. 2C), subsequent detachment (Fig. 2D), muscular infiltration (Fig. 2E) or invasion (Fig. 2F) were noted on day 16, 19, 22, 25 respectively. The different steps were also shown in higher magnification (insets) in the lowest panel. Sections from normal tongue (Fig. 2A,B) indicated proper distribution of epithelium and muscular tissues. We detected tongue metastasis on day 12 in the rvv-lacZ vaccinated mice (data not shown), whereas we did not find tongue metastasis in the PBS treated mice by day 9 when all of them were dead.

Expression of TGF-β1 in the Primary and Metastatic Tumor Lesions

Overexpression of TGF-β1 has been proposed to be associated with increased metastasis and poor prognosis. We therefore compared the expression of TGF-β1 in the primary and metastatic tumors by immunohistochemistry. As shown in Figure 3A, cultured SCCVII/SF cells did not express TGF-β1 at all whereas untreated primary oral tumor secreted abundant TGF-β1 by day 7 (Fig. 3B). In comparison, expression of TGF-β1 was significantly lower in the rvv-IL-2 treated mice on day 16 (Fig. 3C) (+ vs. +++, $P < 0.001$). The number of TGF-β1 positive cells was also low in the rvv-IL-2 vaccinated mice compared to the untreated tumor. We have also examined lymph node and tongue metastatic lesions for TGF-β1 expression. In the metastatic lymph nodes, only infiltrated tumor cells secreted significant amount of TGF-β1 (Fig. 3E,F), but not the lymphocytes surrounding the tumor. Normal lymph node was negative for TGF-β1 expression (Fig. 3D). Insets showed negative or positive tumor cells (arrows) in higher magnification. Similarly, in the metastatic tongue lesions, secretion of TGF-β1 was abundant in the tumor

Fig. 1. Tumor growth and lymph node metastasis in SCCVII/SF tumor bearing C3H/HeJ mice. **A**: Significant tumor regression in the rvv-IL-2 group by day 16 whereas the control groups died by day 12 with large tumors. Tumor growth increased by day 25 in the rvv-IL-2 vaccinated mice. **B**: Lymph node metastasis in the control PBS and rvv-lacZ group by day 9 and 12 respectively involving 4–8 lymph nodes, whereas, lymph node metastasis was detected after day 12 in the rvv-IL-2 vaccinated group involving 1–2 lymph nodes. By day 25, metastasis was detected in all the rvv-IL-2 vaccinated mice involving 5–8 lymph nodes. ●: PBS; ◆: rvv-lacZ; and ●: rvv-IL-2. **C**: Representative photomicrographs showing super cervical, deep cervical and medistinal lymph node metastasis in the rvv-IL-2 vaccinated mice collected on day 25 (magnification ×200). Paraffin embedded 5 μm serial section were stained with Harry's Hematoxyline and Eosine and analyzed for tumor infiltration. Arrows indicate membrane degradation and tumor invasion into the lymph nodes. Insets show typical tumor nests in higher magnification (×400) in the adjacent panel.

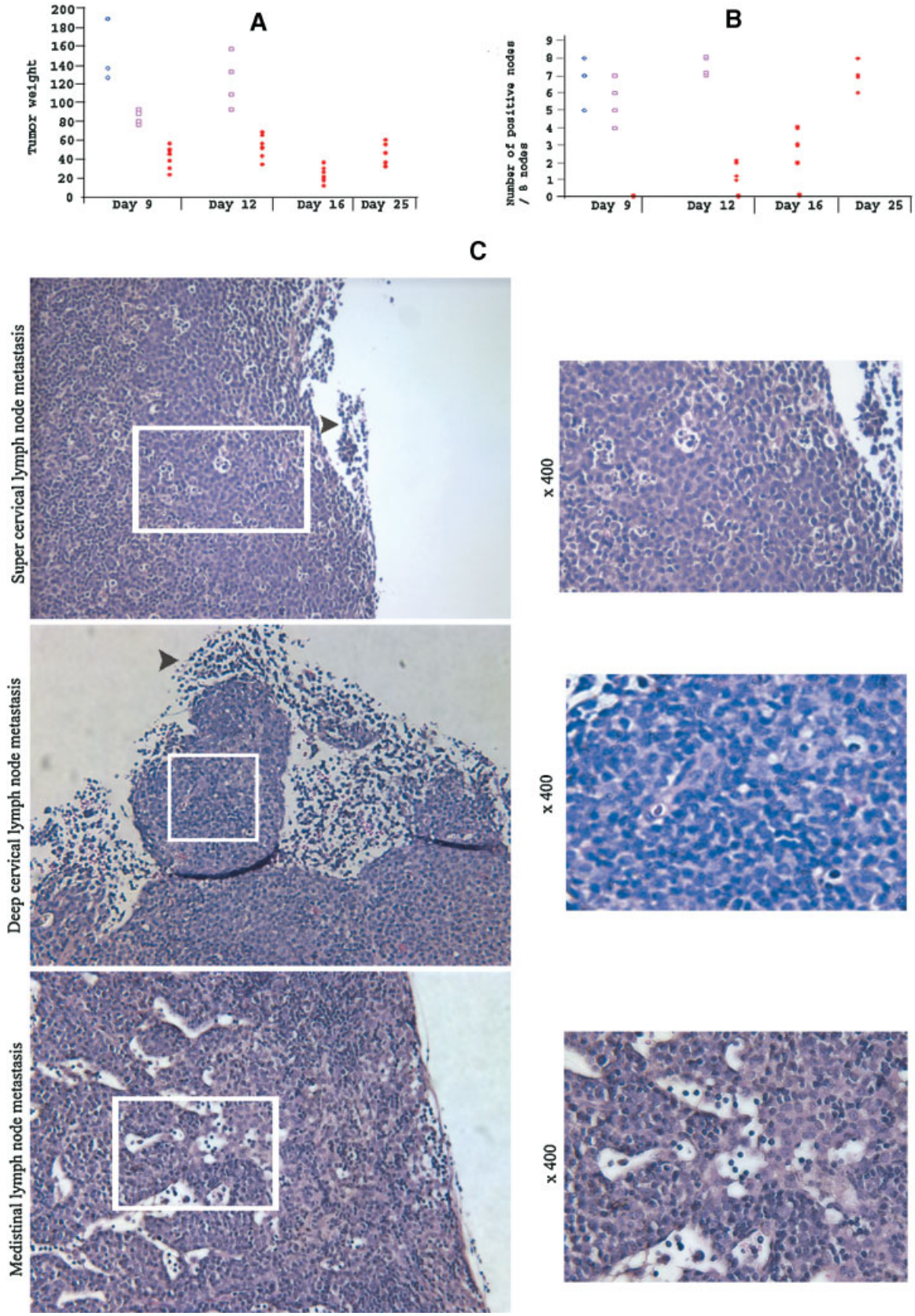
A
Tumor weight
200
180
160
140
120
100
80
60
40
20
0
Day 9
Day 12
Day 16
Day 25
B
Number of positive nodes / 8 nodes
9
8
7
6
5
4
3
2
1
0
Day 9
Day 12
Day 16
Day 25
C
Super cervical lymph node metastasis
Deep cervical lymph node metastasis
Medistinal lymph node metastasis
x 400
x 400
x 400

Fig. 1.

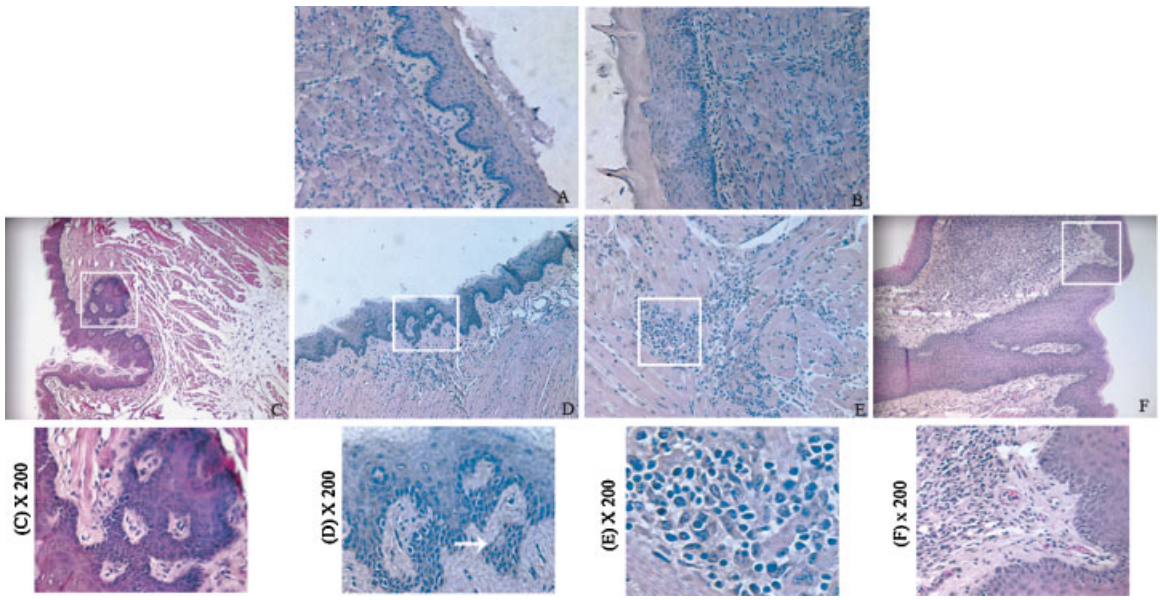

Fig. 2. Tongue metastasis in the rvv-IL-2 vaccinated mice. Tongue tissues from normal and rvv-IL-2 vaccinated mice were collected on day 16, 19, 22, and 25. Tissues were paraffin embedded, sectioned (5 μm) and stained with Harry's Hematoxyline and Eosin. **A**, **B**: Normal tongue epithelium (magnification ×200). **C**–**F**: Invasion of the SCCVII/SF tumor cells through the basement membrane (C), subsequent detachment (D), muscular infiltration (E), or invasion (F) was evident on the above-indicated days respectively (magnification ×100). Higher magnification (×200) of the above stages (insets) are shown in the lowest panel. Arrow indicate invaded and detached tumor nest (D).

microenvironment as well as in the invasive front (Fig. 3J–L). Notably, TGF-β1 expression was evident only in the infiltrating or invasive tumor cells and not in the tumor surrounding normal stroma (Fig. 3J–L). Insets showed positive tumor cell or nest (arrows) in higher magnification. Normal tongue tissues from three different mice used as control were negative for TGF-β1 expression (Fig. 3G,H).

Expression of Active TGF-β1 in Growing Tumor and Secretion of TGF-β1 in the Sera of Tumor-Bearing Mice

In order to determine whether the TGF-β1 present in the tumors was in latent or active form, we performed immunohistochemistry on paraffin embedded sections of primary and tongue metastatic tumors with specific antibodies. All tumors were obtained on day 25. As shown in Figure 4A, both primary and metastatic tumors were negative for staining with latent TGF-β1 antibody (Lap-TGF-β1) whereas high expression was evident for active-TGF-β1 antibody.

Presence of active TGF-β1 may be involved in metastasis of the tumor cells. Therefore, we determined the level of TGF-β1 protein in the sera of tumor-bearing mice on different days after tumor implantation. As shown in Figure 4B, amount of TGF-β1 was significantly higher in the PBS vaccinated mice on day 6 and 9 compared to the rvv-IL-2 vaccinated mice ($P < 0.001$). All PBS mice died by day 9. However, in the rvv-IL2 vaccinated group, TGF-β1 protein level increased steadily from day 12

Fig. 3. Expression of TGF-β1 in the primary tumor, lymph node, and tongue metastasis. Cultured SCCVII/SF tumor cells or paraffin embedded 5 μm serial sections of the primary tumor and tongue metastases were stained with anti-TGF-β1 antibody. The cultured SCCVII/SF cells did not express TGF-β1 (**A**) whereas untreated primary tumor expressed high amounts by day 7 (**B**). Such expression was significantly lower ($P < 0.0001$) in the rvv-IL-2 treated tumor on day 16 (**C**). Normal lymph node was negative for TGF-β1 expression (**D**) whereas such expression was abundant but restricted to the infiltrated tumors in the metastatic super cervical (**E**) or deep cervical (**F**) lymph nodes. Normal TGF-β1 negative lymph node cells or infiltrating tumor cell expressing TGF-β1 (insets) are shown in higher magnification (arrows, ×800). General magnification for A–F was ×200. Normal tongues from three individual mice were negative for TGF-β1 expression (**G**–**I**, magnification ×100), whereas such expression was abundant in the invasive front as well in the tumor microenvironment of day 16 (**J**–**K**, magnification ×200) and day-25 (**L**, magnification ×200) metastatic lesions. Insets shown in higher magnification (×400) indicate expression of TGF-β1 by the infiltrating or invasive tumor cells (Arrows).

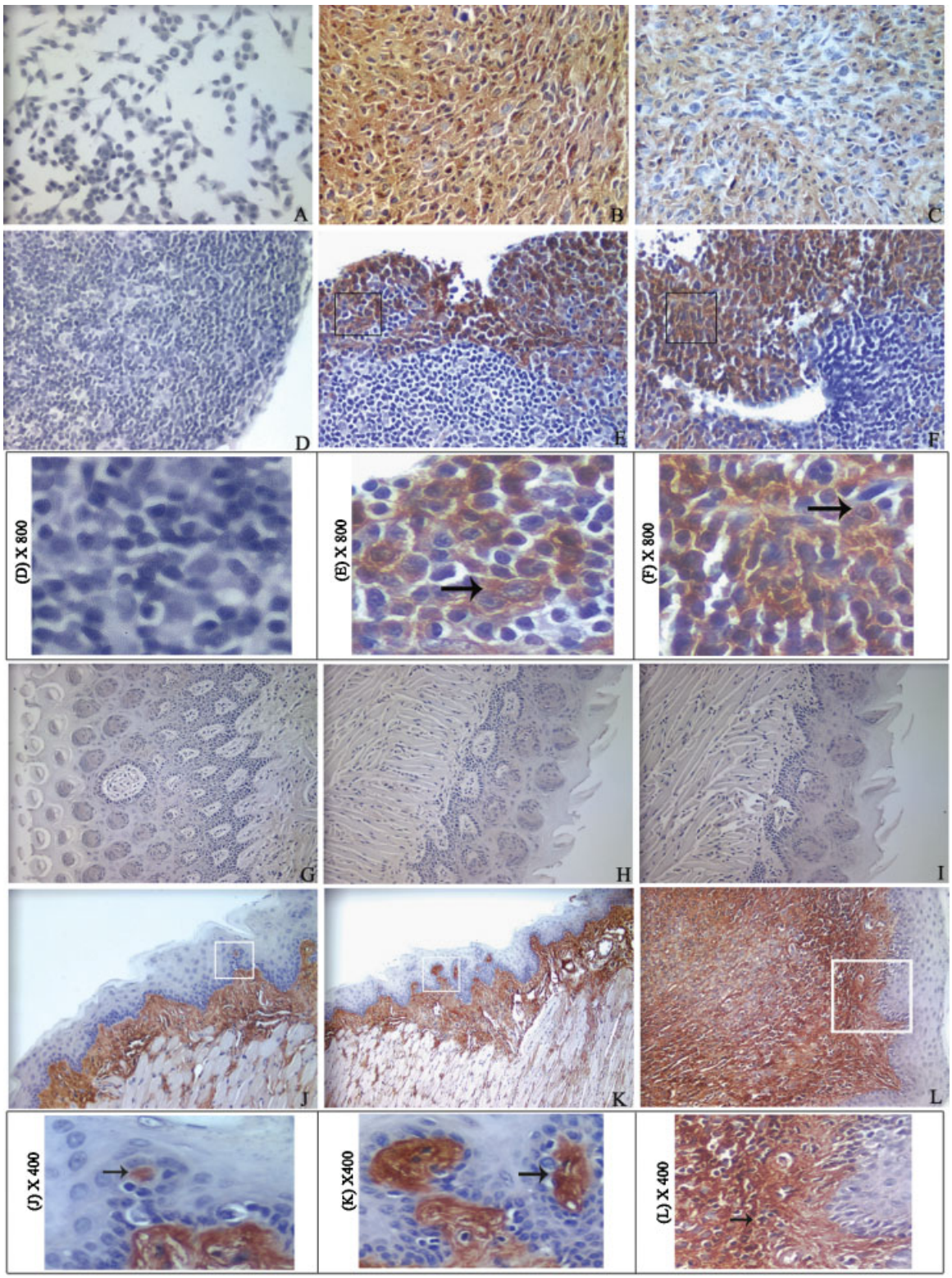

Fig. 3.

onwards (arrow) when metastases into the regional lymph nodes and subsequently to the tongue became evident. In the control naïve mice, amount of TGF-β1 protein was significantly lower ($P < 0.0001$) compared to the PBS or rvv-IL-2 vaccinated mice.

Expression of MT1-MMP, MMP-2, MMP-9, TIMP-1, and TIMP-2 in the Primary Oral Tumor and Tongue Metastasis

Immunostaining was performed on paraffin embedded tumor sections obtained from primary oral tumor and tongue metastases of rvv-IL-2 vaccinated mice on days 16 and 25. Normal tongue was used as control for all the antibodies used. As shown in Figure 5 (panels 1–3), immunoreactivity for MT1-MMP/MMP-2/MMP-9 was significantly higher in the microenvironment as well in the invasive front in both the metastatic tongue lesions compared to the normal control and primary tumor (+ vs. +++, $P < 0.001$). In the day 16 metastatic lesion, invading tumor cells were also positive for MT1-MMP/MMP-2/MMP-9 expression (boxes 1–3 in Fig. 5). The positive cells were also shown in higher magnification (arrows, panel 6 in Fig. 5). Number of MT1-MMP/MMP-2/MMP-9 positive cells and expression was even higher in the day 25 metastatic lesion including the tumor surrounding stroma. On the other hand, immunoreactivity of TIMP-1 and TIMP-2 (panel 4, 5 in Fig. 5) was significantly lower in the tumor microenvironment as well as in the invasive front of the metastatic lesions as well as in the primary tumor compared to the normal control (++ vs. +++, $P < 0.02$). Notably, for both TIMP-1/TIMP-2, reactivity of individual tumor cell in the day 16 (box 4, 5 in panel 6 in Fig. 5) or day 25 lesion (panel 5 in Fig. 5) was lower compared to the normal control. In the day 25 lesion, the tumor surrounding stroma was also negative for TIMP-1/TIMP-2 expression.

Expression of CD31/VEGF-R2/iNOS/E-Cadherin in the rvv Vaccinated Mice

To determine the distribution of blood vessels and status of VEGF-R2, iNOS, and E-cadherin expression, we performed immunohistochemistry on fresh frozen primary and metastatic tumors from rvv-IL-2 vaccinated mice with anti-CD31, anti-VEGF-R2, and anti-iNOS antibodies. Several sections from different regions of the tumor of multiple specimens were examined. As shown in Figure 6A (panel 1), mean vessel density, determined by the number of CD31 positive endothelial cells, was significantly higher in both day 16 and 25 metastatic tongue lesions compared to the primary oral tumor (+++ vs. ++, $P < 0.002$). The mean number of CD31 positive cells was 26 ± 9, 54 ± 8, and 87 ± 11 in the day 16 primary tumor, day 16 and day 25 metastatic lesions respectively. Immunoreactivity of VEGF-R2 (panel 2 in Fig. 6A) and iNOS (panel 3 in Fig. 6A) was significantly higher in both the metastatic lesions compared to the primary oral tumor (+++ vs. +, $P < 0.001$). The number of positive cells for both VEGF-R2 and iNOS was also higher in the metastatic lesions compared to the primary tumor. Expression of E-cadherin was negative in both the tongue metastatic lesions compared to the primary tumor and normal control (panels 1, 2 in Fig. 6B). Expression of E-cadherin was heterogeneous in the primary tumor but did not differ significantly compared to normal control. In the day 25 metastatic lesion (panel 2 in Fig. 6B), expression of E-cadherin by the invaded tumor cells was barely detectable (blue arrow), whereas such expression in the surrounding normal tongue epithelium (white arrow) was comparable to the control.

Real Time RT-PCR of MMPs/TIMPs in the rvv Vaccinated Mice

We performed real-time RT-PCR analysis for the determination of MMP-2, MMP-9, TIMP-1, TIMP-2, and E-cadherin expression with total RNA isolated from the primary and tongue metastasis on days 16 and 25 of rvv-IL-2 vaccinated mice. Before real-time analysis of the target gene, expression of the internal control β-actin gene was normalized in all samples. As shown in Figure 6C, expression of MMP-2 and MMP-9 mRNA was significantly higher in both the metastatic lesions (6.5–8.2 fold) compared to the primary oral tumor (2.6–3.6 fold) and normal control (1.4–1.6 fold) ($P < 0.001$). The difference of expression of MMP-2/MMP-9 between the metastatic lesions was similar ($P > 0.05$). The expression level also did not differ between primary tumor and the normal control ($P > 0.05$) except for MMP-9 (1.6 vs. 3.6 fold, $P < 0.02$). Expression of TIMP-1/TIMP-2 was significantly lower in the primary as well as both the metastatic lesions (2.2–3.7 fold) compared to the normal control (6.9–7.2 fold) ($P < 0.001$). There was no significant difference

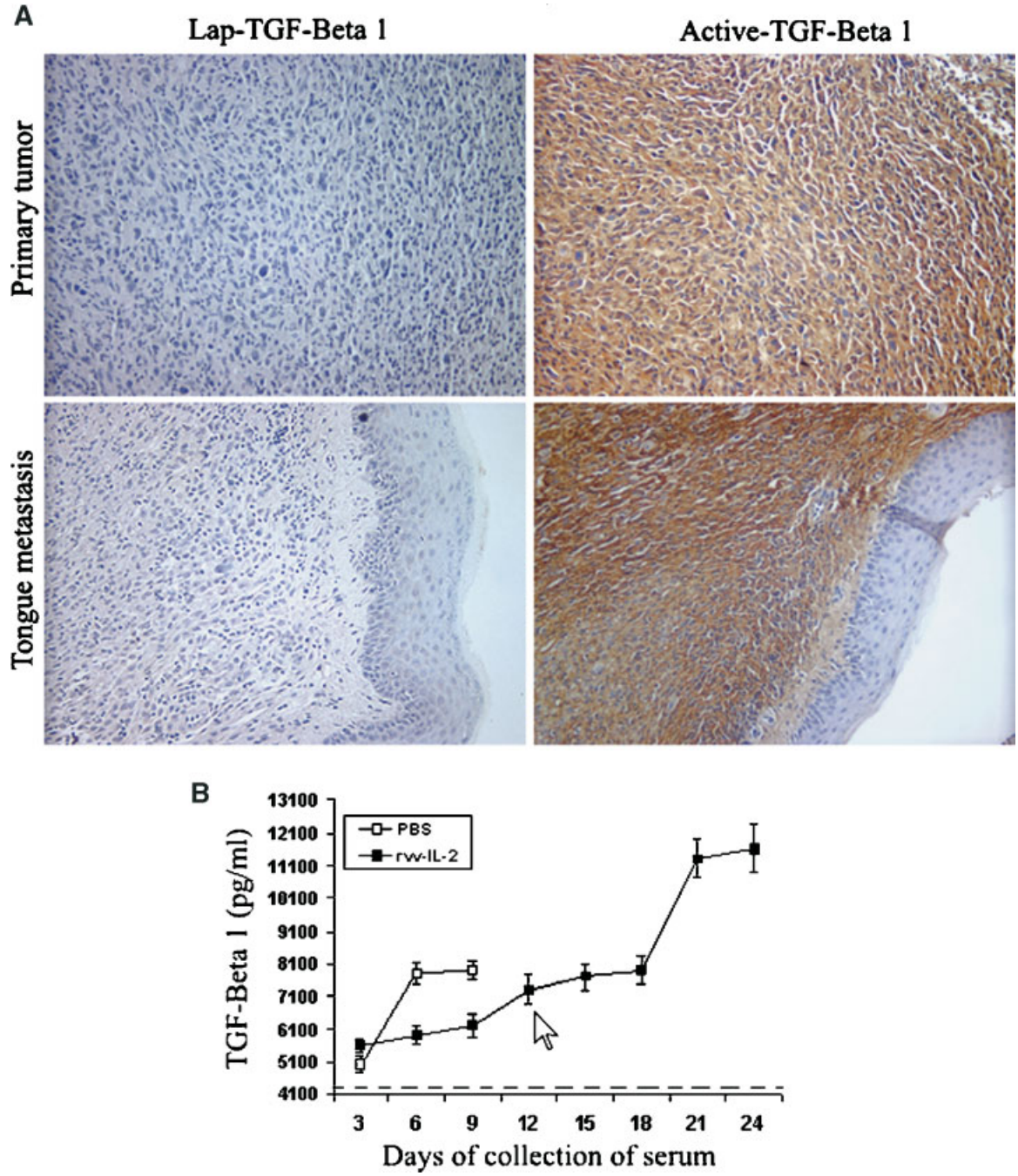

Fig. 4. Expression of TGF β1 in oral tumors and in sera of vaccinated mice. **A**: Paraffin embedded primary and tongue metastatic tumor sections (5 μm) obtained from rvv-IL-2 vaccinated mice on day 25 were stained with latent TGF-β1(Lap-TGF-β1) and active TGF-β1 specific antibodies. Both the primary and tongue metastatic tumors were positive for only active TGF-β1 expression. Magnification ×200. **B**: Sera were obtained from PBS and rvv-IL-2 vaccinated mice on the indicated days after tumor implantation and levels of TGF-β1 were determined by ELISA. Levels of TGF-β1 were significantly higher ($P < 0.001$) in the PBS treated mice on day 6 and 9 compared to those in the rvv-IL-2 group. Level of TGF-β1 increased considerably in the rvv-IL-2 vaccinated mice from day 12 onwards (arrow) when metastases were detected in the lymph nodes and subsequently in the tongue. Sera from naïve mice were used as control (dotted line).

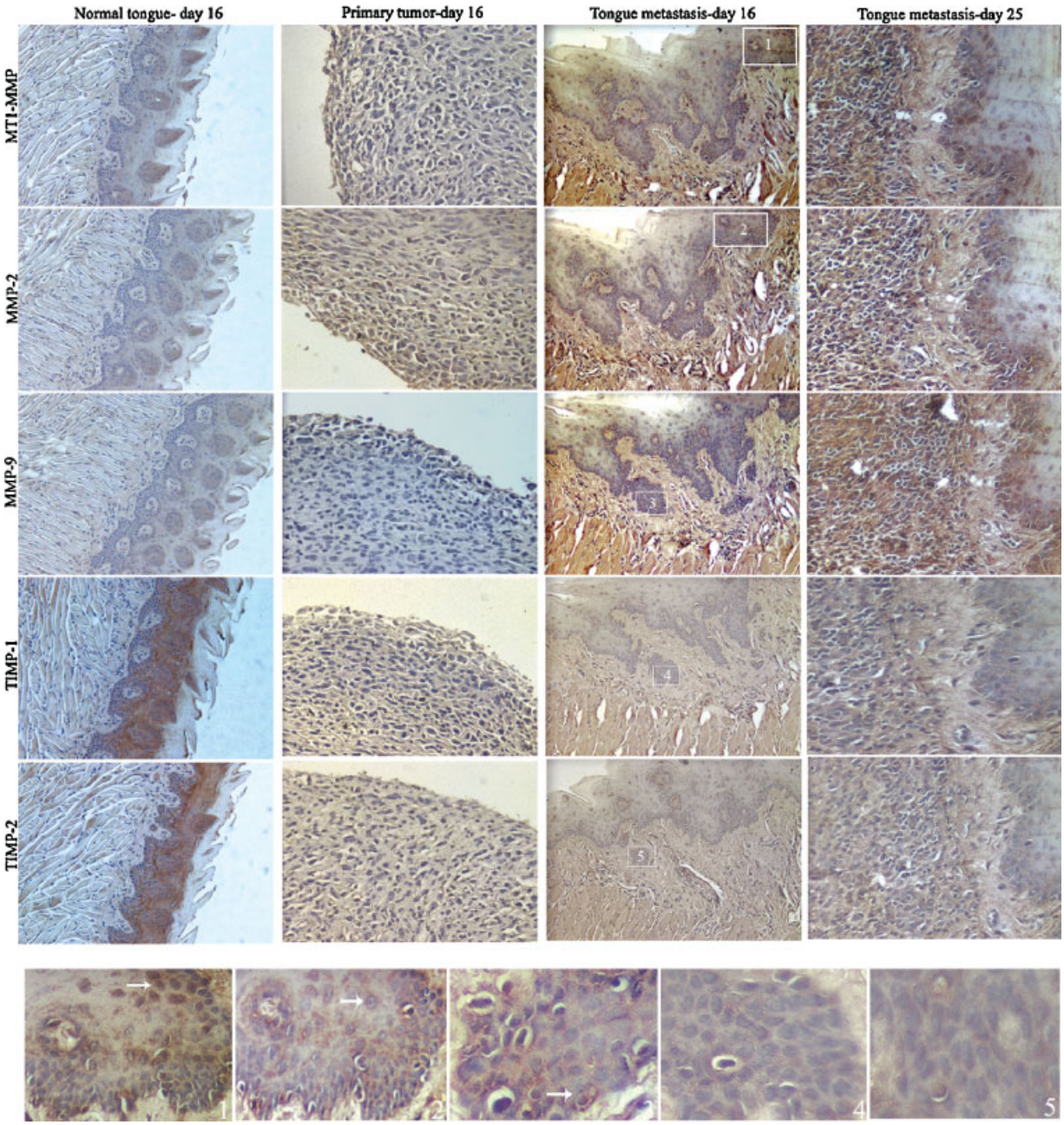

Fig. 5. Expression of MMPs/TIMPs in primary and tongue metastatic tumors in the rvv-IL-2 vaccinated mice. Tumors from the oral cavity, normal or metastatic tongue tissues were collected on the indicated days from the vaccinated mice and paraffin embedded. Five micrometer serial sections were stained with anti-MT1-MMP, MMP-2, MMP-9, TIMP-1, and TIMP-2 antibodies. Normal tongue tissues served as experimental control for each antibody used. Expression of MT1-MMP/MMP-2/MMP-9 was significantly higher in the microenvironment as well in the invasive front in both the metastatic lesions compared to the normal control and primary tumor ($P < 0.001$, **panels 1–3**). Number of MT1-MMP/MMP2/MMP-9 positive cells in the invasive front and surrounding stroma was higher in day 25 metastatic lesion compared to day 16 lesion. Immunoreactivity of TIMP-1 and TIMP-2 was significantly lower in the invasive front and the surrounding stroma of the metastatic lesions as well as in the primary tumor compared to the normal control ($P < 0.02$, **panels 4** and **5**). For both TIMP-1/TIMP-2, reactivity of individual tumor or stromal cell in day 25 metastatic lesion was lower compared to the normal control. General magnification ×200. Boxes 1–3 in **panel 6** show MT1-MMP, MMP-2 (×400), MMP-9 (×600) positive tumor cells (arrow) from day 16 metastatic lesion. Boxes 4 and 5 show TIMP-1/TIMP-2 negative tumor cells from day 16 metastatic lesion (×600).

in expression of the TIMP-1/TIMP-2 genes between primary (3.1–3.2 fold) and the metastatic lesions (2.2–3.7 fold, $P > 0.05$). On the other hand, expression of E-cadherin was significantly lower in the primary (12.5-fold) as well as metastatic tongue lesions (7.2–8.4 fold) compared to the normal control (32-fold) ($P < 0.0001$). There was no difference of E-cadherin mRNA expression between the metastatic lesions ($P > 0.05$), however, such expression was significantly lower in the metastatic lesions compared to the primary tumor ($P < 0.02$).

DISCUSSION

The orthotopic SCCVII/SF murine model resembles human HNSCC in a number of biological properties. Mice bearing SCCVII/SF tumors are immunosuppressed [Qin et al., 2001] and the tumor cells spontaneously metastasize with a pattern similar to human HNSCC [O'Malley et al., 1997]. In this model we tested the efficacy of recombinant vaccinia virus expressing IL-2 as an anti-tumor therapeutic vaccine. The vaccine induced significant tumor regression early on therapy, but its efficacy appeared to be diminished due to recurrent tumor growth and loco-regional metastases.

Metastasis into the regional lymph nodes was the early event in this model (Fig. 1B,C). Eight accessible lymph nodes from several individual mouse of each group was examined carefully to avoid possible over-scoring as they are very small and may be contaminated with tumor cells from the surrounding environment. Moreover, lymph nodes were also cultured to further validate the presence of infiltrating tumor cells. Results presented in Figure 1C clearly demonstrated metastasis of the SCCVII/SF tumor cells into the lymph nodes. Although lymph node infiltration was delayed in the rvv-IL-2 vaccinated mice compared to the control groups, recurrent growth and tumors infiltration into almost all accessible lymph nodes were detectable by day 25. Lymph node infiltration is often associated with loco-regional and distant metastasis in HNSCC [Werner et al., 2002]. In this model, we also detected metastasis of the oral tumor at the tongue as early as day 16 in the rvv-IL-2 vaccinated group. Direct extension of the growing tumor into the tongue instead of metastasis can be ruled out by the results shown in Figure 2. These results clearly demonstrate early invasion of tumor clones into the tongue epithelium followed by subsequent detachment and infiltration or invasion into the muscles. Moreover, we could not detect metastasis in the palate, buccal mucosa or oropharynx regions. These organs would also have been positive if direct extension of the primary tumor took place. Distant organs such as lung, heart, kidney, and other regions also remained free of tumor metastasis during the 25–30 days of tumor development. Thus, early migration of the tumor clones into the regional lymph nodes and subsequently to the tongue appeared to have restricted rvv-IL-2 vaccine efficacy.

TGF-β1, which primarily acts as a tumor suppressor at early stages of carcinogenesis, has also been suggested to promote tumor progression at later stages [Weeks et al., 2001]. In an inducible TGF-β1 expressing skin carcinogenesis model, Weeks et al. [2001] have demonstrated that overexpression of TGF-β1 could induce metastasis by initiating events necessary for invasion, including loss of cell adhesion, early basement membrane degradation, and angiogenesis. It has also been observed in various cancer cells that deregulation of one of the TGF-β signaling components either the receptors or Smads, is sufficient to abolish TGF-β induced growth inhibition. Transfection with the wild type receptors or signaling component in these tumor cells restored TGF-β induced growth arrest [Weeks et al., 2001]. Thus, overexpression of TGF-β1 along with deregulation of the downstream signaling component(s) could potentially induce metastasis at the early stages of tumor progression. In this study, cultured SCCVII/SF tumor cells did not express TGF-β1 at all, but when these cells proliferate into the oral cavity, the tumor cells secreted large amount of TGF-β1 as early as day 7 (Fig. 3). Although in the rvv-IL-2 vaccinated mice, TGF-β1 production was reduced considerably by day 16, the tumor clones metastasize into the lymph nodes and tongue, produced significant amount of TGF-β1 in the tumor microenvironment as well in the invasive front. In this context, it is crucial to determine whether the TGF-β1 in the tumor was in the active or latent form as latency prevents TGF-β1 from binding to ubiquitous cell surface receptors and permits the maintenance of a large extracellular reservoir that can be rapidly accessed by activation [Ehrhart et al., 1997]. Thus, changes in active forms are likely to influence cell phenotype and cell–cell interac-

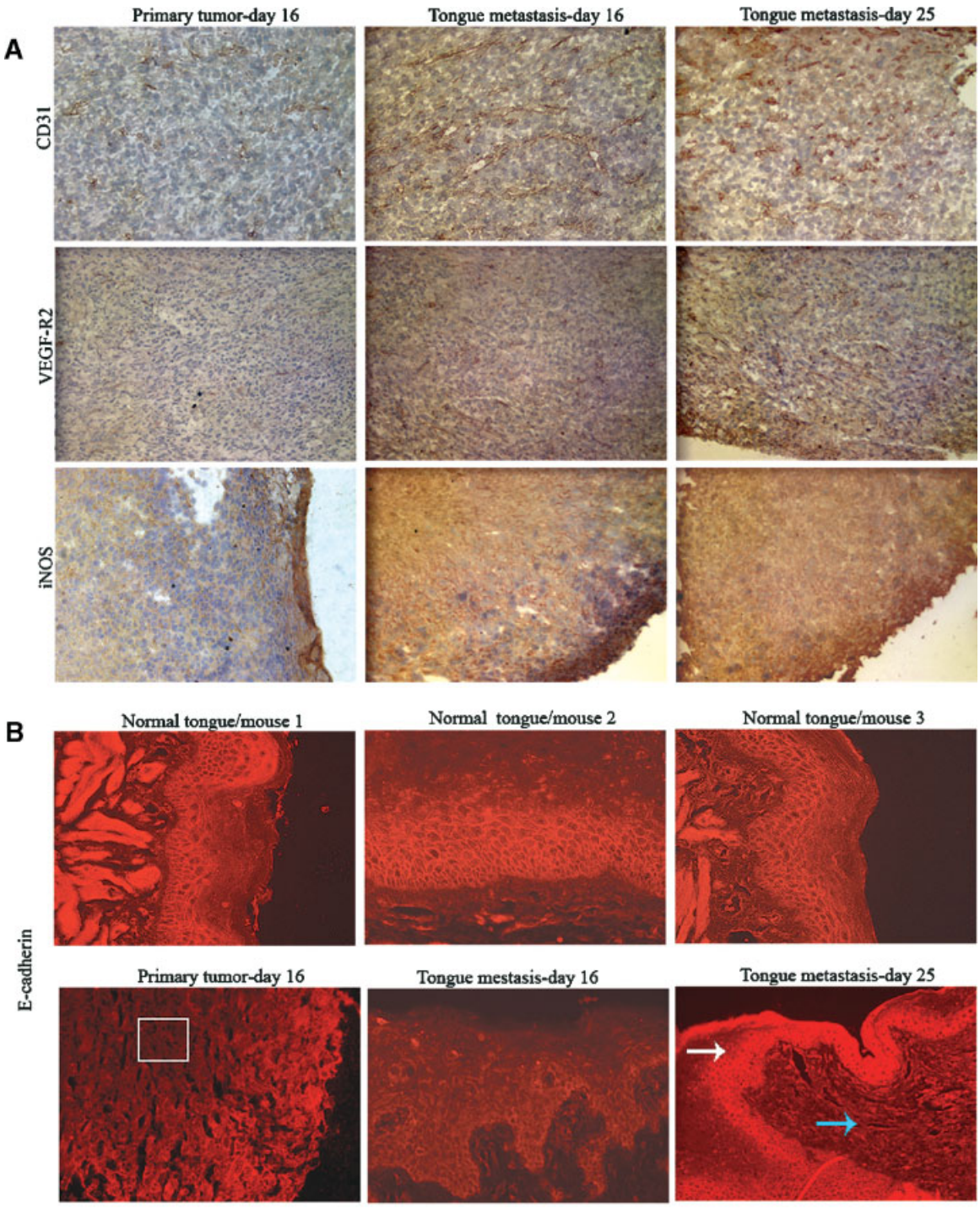
A
Primary tumor-day 16
Tongue metastasis-day 16
Tongue metastasis-day 25
CD31
VEGF-R2
iNOS
B
Normal tongue/mouse 1
Normal tongue/mouse 2
Normal tongue/mouse 3
E-cadherin
Primary tumor-day 16
Tongue mestasis-day 16
Tongue metastasis-day 25
C
Normal Tongue
Primary tumor
Tongue metastasis-day 16
Tongue metastasis-day 25
Relative expression
0
5
10
15
20
25
30
35
40
MMP2
MMP9
TIMP1
TIMP2
E-CADHERIN
Genes analysed

Fig. 6.

tion. Staining with specific antibodies, which can detect both latent and active TGF-β1 protein, indicated that the TGF-β1 was in the active form in both the primary tumor and metastatic lesions (Fig. 4A). Significant amounts of TGF-β1 were also secreted in the sera of rvv-IL-2 vaccinated mice (Fig. 4B). The levels of TGF-β1 in the sera jumped around days 12–16 in the rvv-IL-2 group, when the expression of proteins, such as MMPs, involved in metastasis also started rising. Initiation of metastasis also started at this point. Tumor progression due to immune suppression by TGF-β1 by acting on the T cells is unlikely, since tumor specific helper and cytotoxic T cell activities were almost intact at this time (data not shown). The concurrent rise in the level of TGF-β1 in the sera and initiation of metastasis suggested that secreted TGF-β1 might initiate the cascade leading to tumor metastasis. Moreover, the primary or metastatic SCCVII/SF tumor cells were negative for TGF-βRI/TGF-βRII receptors expression (unpublished data). Thus, it seems likely that other than the Smads, loss of these signaling components might also contribute to TGF-β1 induced tumor metastasis. Factors, which triggered the production of active, TGF-β1 in the growing tumor and the specific time point, and how TGF-β1, concerted the tumors to metastasize remain to be studied.

Detachment of tumor clones from the primary site is a key initiation factor for metastasis into local or distant organs. Decrease or loss in tumor cell adhesion would therefore be the first step for tumor invasion. In this cascade, E-cadherin plays a pivotal role, which in association with catenin maintains normal intercellular adhesion. Several groups have proposed that in carcinomas, E-cadherin functions as an invasive suppressor molecule and thus reduced or loss of E-cadherin may promote detachment and subsequent invasion [Rodrigo et al., 2002]. Increasing evidence also suggest that the disruption of E-cadherin/catenin complex as the cause rather than the consequence of tumor invasion. As depicted in Figure 6C, E-cadherin mRNA expression was significantly reduced in the primary tumor, whereas at the protein level, considerable E-cadherin expression was maintained in different regions of the primary tumor but some clones expressed the protein at very low level (Fig. 6B, white square). This probably indicated the selective growth advantage acquired by the tumor cells to be able to detach and migrate to local or distant organs. Possibly as a result, the metastatic tumor cells in the tongue barely expressed E-cadherin protein. Thus, loss of E-cadherin seemed to be a key initiating event of metastasis in this model.

Once cell motility is changed by the loss of adhesion molecules, the next necessary step for tumor invasion is the degradation of the basement membrane. MMP-2 and MMP-9 degrade type VI collagen, a major component of the basement membrane [Weeks et al., 2001], whereas TIMP-1/TIMP-2 inhibit their function by forming non-covalent complex with them [Werner et al., 2002]. In order to understand the role of MMPs/TIMPs expression, we performed real-time RT-PCR as well as immunohistochemical analysis at different stages of tumor growth in the rvv-IL-2 vaccinated mice. At the

Fig. 6. Expression of CD31/VEGF-R2/iNOS/E-cadherin protein and mRNA of MMP-2, MMP-9, TIMP-1, TIMP-2, and E-cadherin in the primary and metastatic tumors of the rvv-IL-2 vaccinated mice. Fresh frozen serial tumor sections (5 μm) from the oral cavity and metastatic tongue tissues were collected on the indicated days and stained with anti-CD31, VEGF-R2, and iNOS antibodies. **A**: Number of CD31 positive endothelial cells was significantly higher ($P < 0.002$) in both day 16 and 25 tongue metastatic lesions compared to the primary oral tumor. Immunoreactivity of VEGF-R and iNOS was also significantly higher ($P < 0.001$) in both the metastatic lesions compared to the primary oral tumor. **B**: Expression of E-cadherin was significantly lower ($P < 0.001$) in both the tongue metastatic lesions compared to the primary tumor and normal control. Expression was heterogeneous in the primary tumor but did not differ significantly compared to normal control (**panel 2**). White square indicate low E-cadherin expression by the tumor cells. In day 25 metastatic lesion, expression of the tumor surrounding normal tongue epithelium was strong like the normal control (white arrow) whereas invaded tumor was negligible for E-cadherin expression (Blue arrow). Magnification ×200. **C**: Expression of MMP-2 and MMP-9 mRNA was significantly higher in both the metastatic lesions compared to the primary oral tumor and control ($P < 0.0001$). There was no difference of MMP-2/MMP-9 expression between the metastatic lesions ($P > 0.05$). The expression level also did not differ significantly between primary tumor and the control except for MMP-9. Expression of TIMP-1/TIMP2 was significantly lower in the primary as well as both the metastatic lesions compared to the control ($P < 0.001$). There was no difference in expression of the TIMP-1/TIMP-2 mRNA between primary tumor and the metastatic lesions ($P > 0.05$). Expression of E-cadherin was significantly lower in the primary as well as metastatic tongue lesions compared to control ($P < 0.001$). There was no difference of E-cadherin mRNA expression between the metastatic lesions ($P > 0.05$), however, E-cadherin expression was significantly lower in the metastatic lesions compared to the primary tumor ($P < 0.04$). *$P < 0.05$ versus the normal tongue; + $P < 0.05$ versus the primary tumor.

mRNA level, significant expression MMP-2/MMP-9 in the tongue metastatic lesions suggested their possible role in the degradation of the basement membrane and tumor invasion (Fig. 6C). On the other hand, lower mRNA expression of TIMP-1/TIMP-2 in the metastatic lesions suggested a favorable microenvironment for MMP-2 and MMP-9 mediated tumor progression. Particularly, loss of TIMP-2 could greatly facilitate tumor invasive phenotype as they can directly inhibit MMPs action [Werner et al., 2002]. To compare the expression at protein level, we performed immunohistochemistry. Immunohistochemistry has several advantages. It allows direct correlation with morphology and it can be performed on fresh frozen or paraffin embedded specimen [Franchi et al., 2002]. Thus, it is practical for routine assessment of MMPs in diagnostic practice [Franchi et al., 2002]. However, it has been suggested that immunohistochemistry cannot distinguish between latent MMPs and active forms [Curran and Murray, 1999]. Conversely, other techniques like zymography or quenched fluorescent substrate hydrolysis separate the active and latent forms of MMPs, but they do not allow correlation with morphology [Franchi et al., 2002]. In our study, the expression of MMPs was found largely in the invasive front as well as in the tumor microenvironment of the metastatic tongue lesions, possibly to facilitate tumor invasion into the muscle (panels 1–3 in Fig. 5). But it was not clear which cell type in particular secreted the MMPs in the early metastatic lesion except for some infiltrating tumor cells (panel 6 in Fig. 5), whereas at the later stages, tumor cells were found to produce large amount of MMPs. Adjacent stromal cells in the late stage metastatic lesion also secreted MMPs, suggesting a contribution of host-derived proteinases to tumor progression [McCawley and Matrisian, 2001]. Significant expression of MT1-MMP was notable in the metastatic lesions, since these can activate other MMPs, especially MMP-2 [Werner et al., 2002], co-expression of MMP-2 and MT1-MMP might have contributed significantly in the initiation of tumor invasion. Similarly, higher expression of MMP-9 by the tumor cells in the later stages of metastatic formation indicated its possible role in angiogenesis, since MMP-9 has been reported to be an important molecule involved in angiogenesis [Werner et al., 2002; Lu et al., 2004a]. Lower expression of TIMP-1 and TIMP-2 in the metastatic lesions might have contributed to the loss of protective function of these MMP inhibitors, which lead to tumor progression (Figs. 5 and 6). Lower TIMP-1 levels in metastatic oral squamous cell carcinoma have been reported [Werner et al., 2002; Lu et al., 2004a], however, the specific role of TIMP-2 in HNSCC progression further needs to be addressed. As shown in Figure 5, probably a high ratio of MMPs/TIMP-2 expression in the tumor microenvironment as well as in the invasive front of the tumor favored tumor invasion. The immunohistochemical data presented here correlated well with our real-time RT-PCR analysis.

Loss of cell adhesion and degradation of the basement membrane are required to initiate local invasion, whereas increased angiogenesis is essential for autonomous tumor growth and distant metastasis [Weeks et al., 2001]. In the process of angiogenesis, MMPs play a pivotal role, because these enzymes degrade the ECM and provide a permissive microenvironment for the growth of new blood vessels [Franchi et al., 2002]. In this context, MMP-9 has been found to be an important regulator of angiogenesis in HNSCC that cooperates with other factors such as iNOS and VEGF-R2 expression in supporting the process of neovascularization [Basu et al., 2001; Franchi et al., 2002; Werner et al., 2002]. In the present study, increased vessel formation, significant expression of VEGF-R2 and iNOS correlated well with the MMP-9 overexpression in the metastatic lesions.

The current study suggested that active TGF-β1 production might be involved in the process of metastasis in association with MMPs and the pro-angiogenic molecules at different stages of tumor progression. It appears that down regulation of the expression of TGF-β1 using suitable antagonists could be useful for preventing metastasis in this model. Since TGF-β1 is involved in multiple biological processes, systemic down regulation of TGF-β1 is not desirable. Local expression of TGF-β1 at the tumor site can be controlled by TGF-β1 antagonists such as soluble receptors of TGF-β1. This can be done by using recombinant vaccinia virus. Experiments are underway to explore this possibility.

REFERENCES

Basu S, Nagy JA, Pal S, Vasile E, Eckelhoefer IA, Bliss VS, Manseau EJ, Dasgupta PS, Dvorak HF, Mukhopadhyay

D. 2001. The neurotransmitter dopamine inhibits angiogenesis induced by vascular permeability factor/vascular endothelial growth factor. Nat Med 7:569–574.

Chambers AF, Matrisian LM. 1997. Changing views of the role of matrix metalloproteinases in metastasis. J Natl Cancer Inst 89:1260–1270.

Curran S, Murray GI. 1999. Matrix metalloproteinases in tumour invasion and metastasis. J Pathol 189:300–308.

Dasgupta S, Tripathi PK, Bhattacharya-Chatterjee M, O'Malley B, Jr., Chatterjee SK. 2003. Recombinant vaccinia virus expressing IL-2 generates effective antitumor responses in an orthotopic murine model of head and neck carcinoma. Mol Ther 8:238–248.

Dasgupta S, Bhattacharya-Chatterjee M, O'Malley BW, Jr., Chatterjee SK. 2004. Reversal of immune suppression following vaccination with recombinant vaccinia virus expressing IL-2 in an orthotopic murine model of head and neck squamous cell carcinoma. Cancer Ther 2: 375–388.

De Stefani A, Forni G, Ragona R, Cavallo G, Bussi M, Usai A, Badellino F, Cortesina G. 2002. Improved survival with perilymphatic interleukin 2 in patients with resectable squamous cell carcinoma of the oral cavity and oropharynx. Cancer 95:90–97.

Edwards BK, Howe HL, Ries LA, Thun MJ, Rosenberg HM, Yancik R, Wingo PA, Jemal A, Feigal EG. 2002. Annual report to the nation on the status of cancer, 1973–1999, featuring implications of age and aging on U.S. cancer burden. Cancer 94:2766–2792.

Ehrhart EJ, Segarini P, Tsang ML, Carroll AG, Barcellos-Hoff MH. 1997. Latent transforming growth factor beta1 activation in situ: Quantitative and functional evidence after low-dose gamma-irradiation. FASEB J 11:991–1002.

Franchi A, Santucci M, Masini E, Sardi I, Paglierani M, Gallo O. 2002. Expression of matrix metalloproteinase 1, matrix metalloproteinase 2, and matrix metalloproteinase 9 in carcinoma of the head and neck. Cancer 95: 1902–1910.

Ginos MA, Page GP, Michalowicz BS, Patel KJ, Volker SE, Pambuccian SE, Ondrey FG, Adams GL, Gaffney PM. 2004. Identification of a gene expression signature associated with recurrent disease in squamous cell carcinoma of the head and neck. Cancer Res 64:55–63.

Hofmann UB, Eggert AA, Blass K, Brocker EB, Becker JC. 2003. Expression of matrix metalloproteinases in the microenvironment of spontaneous and experimental melanoma metastases reflects the requirements for tumor formation. Cancer Res 63:8221–8225.

Huang S, Pettaway CA, Uehara H, Bucana CD, Fidler IJ. 2001. Blockade of NF-kappaB activity in human prostate cancer cells is associated with suppression of angiogenesis, invasion, and metastasis. Oncogene 20:4188–4197.

Kim MH, Kitson RP, Albertsson P, Nannmark U, Basse PH, Kuppen PJ, Hokland ME, Goldfarb RH. 2000. Secreted and membrane-associated matrix metalloproteinases of IL-2-activated NK cells and their inhibitors. J Immunol 164:5883–5889.

Kim ES, Kies M, Herbst RS. 2002. Novel therapeutics for head and neck cancer. Curr Opin Oncol 14:334–342.

Li D, Jiang W, Bishop JS, Ralston R, O'Malley BW, Jr. 1999. Combination surgery and nonviral interleukin 2 gene therapy for head and neck cancer. Clin Cancer Res 5:1551–1556.

Lu KV, Jong KA, Rajasekaran AK, Cloughesy TF, Mischel PS. 2004a. Upregulation of tissue inhibitor of metalloproteinases (TIMP)-2 promotes matrix metalloproteinase (MMP)-2 activation and cell invasion in a human glioblastoma cell line. Lab Invest 84:8–20.

Lu SL, Reh D, Li AG, Woods J, Corless CL, Kulesz-Martin M, Wang XJ. 2004b. Overexpression of transforming growth factor beta1 in head and neck epithelia results in inflammation, angiogenesis, and epithelial hyperproliferation. Cancer Res 64:4405–4410.

McCawley LJ, Matrisian LM. 2001. Tumor progression: Defining the soil round the tumor seed. Curr Biol 11: R25–R27.

Nagase H. 1997. Activation mechanisms of matrix metalloproteinases. Biol Chem 378:151–160.

O'Malley BW, Jr., Cope KA, Johnson CS, Schwartz MR. 1997. A new immunocompetent murine model for oral cancer. Arch Otolaryngol Head Neck Surg 123:20–24.

Qin H, Chatterjee SK. 1996. Recombinant vaccinia expressing interleukin-2 for cancer gene therapy. Cancer Gene Ther 3:163–167.

Qin H, Valentino J, Manna S, Tripathi PK, Bhattacharya-Chatterjee M, Foon KA, O'Malley BW, Jr., Chatterjee SK. 2001. Gene therapy for head and neck cancer using vaccinia virus expressing IL-2 in a murine model, with evidence of immune suppression. Mol Ther 4:551–558.

Rodrigo JP, Dominguez F, Alvarez C, Manrique C, Herrero A, Suarez C. 2002. Expression of E-cadherin in squamous cell carcinomas of the supraglottic larynx with correlations to clinicopathological features. Eur J Cancer 38: 1059–1064.

Sauter ER, Nesbit M, Watson JC, Klein-Szanto A, Litwin S, Herlyn M. 1999. Vascular endothelial growth factor is a marker of tumor invasion and metastasis in squamous cell carcinomas of the head and neck. Clin Cancer Res 5: 775–782.

Trudel D, Fradet Y, Meyer F, Harel F, Tetu B. 2003. Significance of MMP-2 expression in prostate cancer: An immunohistochemical study. Cancer Res 63:8511–8515.

Weeks BH, He W, Olson KL, Wang XJ. 2001. Inducible expression of transforming growth factor beta1 in papillomas causes rapid metastasis. Cancer Res 61: 7435–7443.

Werner JA, Rathcke IO, Mandic R. 2002. The role of matrix metalloproteinases in squamous cell carcinomas of the head and neck. Clin Exp Metastasis 19:275–282.

Yang YA, Dukhanina O, Tang B, Mamura M, Letterio JJ, MacGregor J, Patel SC, Khozin S, Liu ZY, Green J, Anver MR, Merlino G, Wakefield LM. 2002. Lifetime exposure to a soluble TGF-beta antagonist protects mice against metastasis without adverse side effects. J Clin Invest 109:1607–1615.